Multiple quasi-phase-matching in nonlinear Raman–Nath diffraction

Andrey M. Vyunishev[1,2,*] and Anatoly S. Chirkin[3]

[1]*L.V. Kirensky Institute of Physics, 660036 Krasnoyarsk, Russia*

[2]*Siberian Federal University, 660079 Krasnoyarsk, Russia*

[3]*Faculty of Physics and International Laser Center, M. V. Lomonosov Moscow State University, 119992 Moscow, Russia*

**Corresponding author: vyunishev@iph.krasn.ru*

Received January 13, 2015; revised February 18, 2015; accepted February 18, 2015;
posted February 23, 2015 (Doc. ID 232126); published March 20, 2015

The method of the superposition of a nonlinearity modulation is employed to design a two-dimensional (2D) nonlinear photonic lattice for efficient multiple quasi-phase-matched second harmonic generation in the process of nonlinear Raman–Nath diffraction (NRND). An analytical solution is proposed to calculate the second harmonic intensity in rectangular 2D lattices. This approach can be useful for the generation of multiple second harmonic beams with the efficiency a few orders of magnitude higher than in the case of nonphase-matched generation via NRND.

OCIS codes: (190.2620) Harmonic generation and mixing; (190.4223) Nonlinear wave mixing; (190.4420) Nonlinear optics, transverse effects in.

http://dx.doi.org/10.1364/OL.40.001314

Nonlinear Raman–Nath diffraction (NRND) is the most exciting nonlinear optical phenomenon to occur in periodic nonlinear photonic lattices [1–6]. This phenomenon appears as multiple second harmonic beams generated at small angles with respect to the incoming fundamental frequency (FF) beam, which is defined by the lattice periodicity [2]. However, NRND is inherently a non-phase-matched nonlinear optical process, which limits its applications [7]. This inherent limitation could be overcome by using two-dimensional (2D) nonlinear photonic lattices [8]. In [9], it was reported that the generalization of the conventional quasi-phase-matching (QPM) technique to fit the case of 2D nonlinear photonic lattices could be used to obtain efficient, multiple second harmonic generations (SHG) in the process of Cerenkov nonlinear diffraction. In contrast, the use of the QPM technique in the case of NRND is complicated, because different orders have specific phase mismatches. Despite this, a modification of the QPM technique could help solve the problem. It has been reported [10] that random QPM can be employed to increase SHG efficiency. However, in this case, the appropriate reciprocal lattice vectors have arbitrary Fourier amplitudes in a wide range, and the conversion efficiencies are not high enough. Another way of increasing the efficiency of the SHG is to apply the method known as the superposition of nonlinearity modulation [11]. This method makes it possible to design a nonlinear photonic lattice that provides a set of desired reciprocal lattice vectors for multiple nonlinear optical processes. This is the most suitable method for the realization of multiple SHG via NRND. In this case, specific phase mismatches corresponding to different NRND orders are compensated for by the appropriate reciprocal lattice vectors with the Fourier amplitudes as high as possible.

In this Letter, we report our theoretical studies on the NRND in one- and two-dimensional nonlinear photonic lattices. We propose a strategy to increase SHG efficiency based on the method of the superposition of quadratic nonlinearity modulation. This method enables us to achieve efficient quasi-phase-matched SHG for several NRND orders simultaneously.

Let us consider the SHG in the one-dimensional (1D) and 2D nonlinear photonic lattices presented in Fig. 1. We will introduce a $g(x,y)$ function that describes the 2D space variance of the nonlinear coefficient over the lattices and takes the values 1 or −1. This function can be represented as the multiplication of two functions, each one corresponding to one space dimension. such that $g(x,y) = \xi(x)\eta(y)$.

Let us specify function $\eta(y)$ as a superposition of harmonic oscillations:

$$\eta(y) = \mathrm{sgn}\left[\sum_j C_j \sin(G_{Yj}y + \varphi_j)\right], \tag{1}$$

where C_j, G_{Yj}, and φ_j are the numerical coefficient, the primary reciprocal lattice vector, and the phase, respectively. The signum function can be defined as $\mathrm{sgn}(x) = |x|/x$. Hereafter, we will refer to either the periodic or aperiodic 2D lattices shown in Figs. 1(b) and 1(c), depending on the type of the function $\eta(y)$.

In accordance with [7,12], the second harmonic field amplitude at the distance L in a 1D lattice ($g(x,y) = \xi(x)$) shown in Fig. 1(a) is governed by

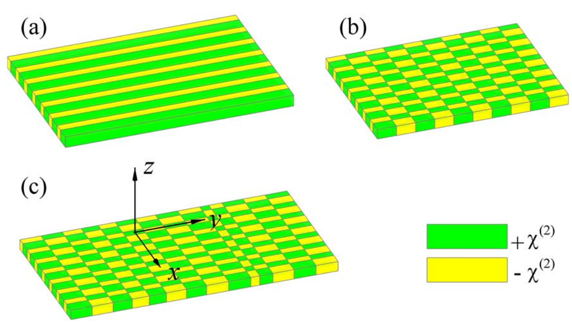

Fig. 1. Design of periodic 1D (a) and 2D (b) nonlinear photonic lattices and aperiodic 2D (c) one.

$$A_2(K_X, L) = \alpha \exp(iLK_X^2/2k_2) \int_0^L R(K_X) \exp(i\Delta\tilde{k}y)\mathrm{d}y, \quad (2)$$

where $\alpha = \pi a^2 \Gamma/2$, $\Gamma = -i\beta_2 I_1$, $\beta_2 = 2\pi k_2 \chi^{(2)}/n_2^2$, $\Delta\tilde{k} = \Delta k - K_X^2/2k_2$, $\Delta k = k_2 - 2k_1$ is the wave vector mismatch between the FF and second harmonic waves, n_2 is the refractive index at the second harmonic frequency, $\chi^{(2)}$ is the quadratic nonlinear susceptibility, and K_X is the spatial frequency. The function $R(K_X) = \sum_m \xi_m \exp[-a^2(mG_X + K_X)^2/8]$ is responsible for phase matching the transverse components of the FF and second harmonic wave vectors, which produces a series of second harmonic beams propagating at the angles $\theta_m = \arcsin(mG_X/k_2)$. Here, $m = 0, \pm 1, \pm 2, \ldots$ is the NRND order, G_X is the primary reciprocal lattice vector, and a is the FF beam radius. The Fourier coefficients ξ_m for a periodic function with the duty cycle D take the form $\xi_m = 2D - 1$ if $m = 0$ and $\xi_m = 2\sin(\pi m D)/\pi m$ otherwise. For the calculations, we consider extraordinary waves that are coupled by the relevant nonlinear coefficient of congruent lithium niobate d_{33}, i.e., $\chi^{(2)} = 2d_{33}$. The required refractive index data were taken from [13]. For the second harmonic amplitude generated in a 1D lattice, the integration of Eq. (2) gives

$$A_2(K_X, L) = \alpha L \exp(iL/2(\Delta k + K_X^2/2k_2)) \times \mathrm{sinc}(\Delta\tilde{k}L/2) R(K_X), \quad (3)$$

where $\mathrm{sinc}(x) = \sin(x)/x$.

The expression given in Eq. (2) can be easily generalized to the case of a 2D lattice using the approach from [14–16]. In this case, the 2D lattice can be represented as a stack of 1D lattices arranged together along the y direction as depicted in Figs. 1(b) and 1(c). Each 1D lattice represents a layer contributing to the SHG. The function $\xi(x)$ of a given layer is an inverse duplicate of the adjacent layers. We assume that the qth layer of thickness d_q is constrained by positions y_{q-1} and y_q, so that $y_q = y_{q-1} + d_q$ $(y_0 = 0)$. The function $\eta(y)$ provides a set of positions y_q, where the sign of nonlinear susceptibility alternates. Then, by calculating the second harmonic amplitudes layer by layer, one can obtain the total second harmonic field amplitude at the exit of the lattice. Consequently, the second harmonic field amplitude after N layers is expressed as follows:

$$\begin{aligned} A_2(K_X, y_q) &= -(i\alpha/\Delta\tilde{k}) R(K_X) \exp(iLK_X^2/2k_2) \\ &\quad \times \sum_{q=1}^{N} (-1)^q (\exp(i\Delta\tilde{k}y_q) - \exp(i\Delta\tilde{k}y_{q-1})) \\ &= -(i\alpha/\Delta\tilde{k}) R(K_X) \exp(iLK_X^2/2k_2) \\ &\quad \times \sum_{q=1}^{N} (-1)^q \exp(i\Delta\tilde{k}\vartheta_q)(\exp(i\Delta\tilde{k}d_q) - 1). \quad (4) \end{aligned}$$

The factor $(-1)^q$ accounts for the phase flip at the transition from one layer to another, while the factor $\exp(i\Delta\tilde{k}\vartheta_q)$ accounts for the relative phase accumulated at the distance $\vartheta_q = \sum_{r=1}^{q-1} d_r$. The second harmonic spectral intensity is given by $S(K_X) = |A_2(K_X)|^2$.

First, we analyze SHG via NRND in a 1D nonlinear photonic lattice. In this case, we use Eq. (3). For the calculations, the following parameters were taken: the FF wavelength of 1.545 μm, the focal spot radius $a = 17$ μm, the lattice period of 10 μm, the duty cycle $D = 0.75$, and the sample length of 1 mm. Under these conditions, the second harmonic intensity corresponding to different transverse orders m oscillates along the media, as shown in Fig. 2(a). The period of oscillations grows with the order m until it maximizes at the fifth order. This is due to the nonmonotonic behavior of the absolute value of $\Delta\tilde{k}$ presented in Fig. 3(a). Note that as the propagation distance increases, the angular intensities in Fig. 2(a) shift toward larger angles for the first five orders, in contrast to the sixth one. There is a range of sample thicknesses and propagation angles where an odd number of coherent lengths falls within the propagation direction of SHG. In that case, maximum nonphase-matched SHG takes place. This situation is similar to the Maker fringes observed in homogeneous nonlinear media away from phase matching. The angular shift of the maxima of the second harmonic intensity in Fig. 2(a) is caused by the term under the sinc function in Eq. (3).

In Fig. 2(b), the growth in second harmonic intensity for the fifth and sixth NRND orders with respect to the lower ones is due to the contribution from the sinc function in Eq. (3). This factor has maximum effect when Cerenkov's radiation condition $k_2 \cos(\theta_C) = 2k_1$ is fulfilled; for our case, the external Cerenkov second harmonic angle is $\theta_C = 24.88$ deg. The Cerenkov angle lies between the angles of the fifth and sixth NRND orders considered by the function $R(K_X)$ in Eq. (3). As a result,

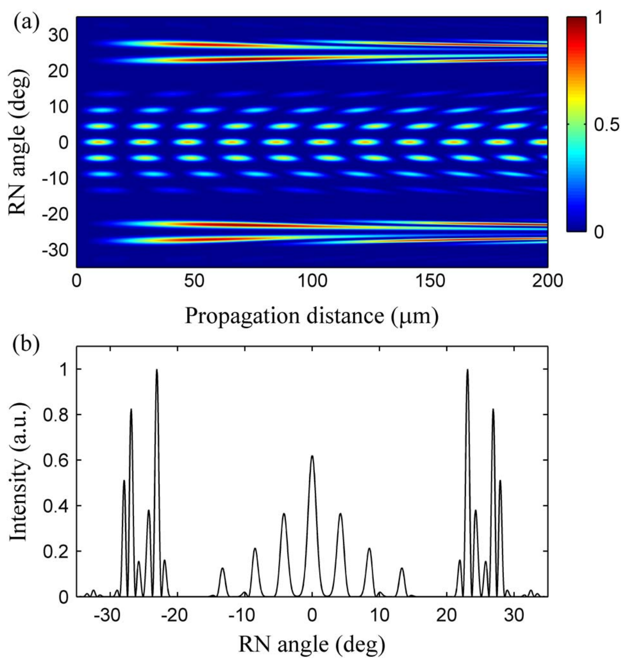

Fig. 2. Angular dependence of second harmonic intensity as a function of (a) the propagation distance and (b) the angular distribution of the second harmonic intensity at the distance $L = 200$ μm in a 1D nonlinear photonic lattice.

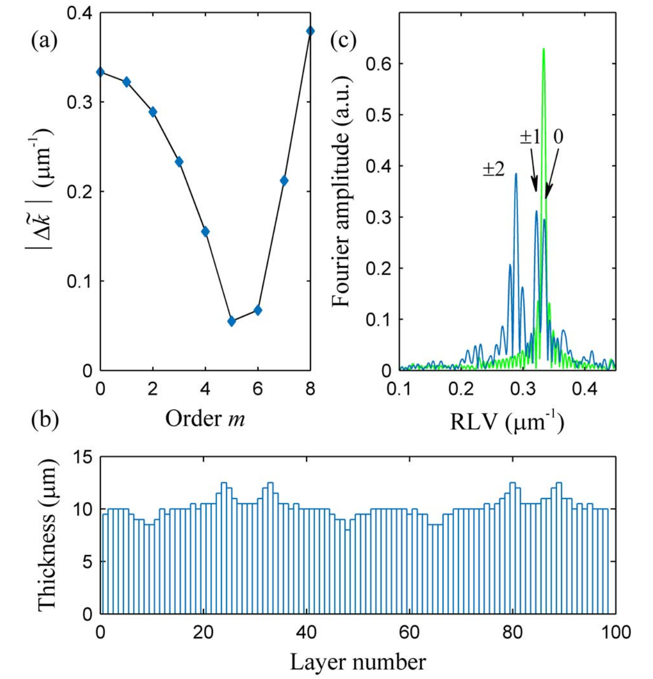

Fig. 3. (a) Absolute value of the wave vector mismatch versus the transverse QPM order. (b) Layer thickness as a function of the layer numbers in the direction y. (c) Reciprocal lattice vector spectra of the periodic (green) and aperiodic (blue) function $\eta(y)$.

angular oscillations in the second harmonic intensity exist in the range from 20 to 30 deg.

When analyzing SHG in 2D nonlinear photonic lattices, we can refer to either single or multiple QPM, depending on how many transverse QPM orders are supposed to be simultaneously matched by the reciprocal lattice vectors provided by the lattice in the longitudinal direction. We assume that all longitudinal components of FF and second harmonic wave vectors are matched by the primary reciprocal lattice vector, resulting in the first-order QPM for all NRND orders involved.

We consider multiple QPM interactions of the first three transverse orders ($m = 0, \pm1, \pm2$), although the method used could be applied to an arbitrary number of orders. For definiteness, we assume that indexes j in Eq. (1) correspond to indexes m in Eq. (4), i.e., $j = |m|$. Then,

$$G_{Ym} = |\Delta\tilde{k}(m)| = \Delta k - (mG_X)^2/2k_2. \tag{5}$$

Under this assumption, an aperiodic 2D lattice must contain the reciprocal lattice vectors $G_{Y,0} = \Delta k$, $G_{Y,1} = \Delta k - G_{X,1}^2/2k_2$, and $G_{Y,2} = \Delta k - 4G_{X,1}^2/2k_2$. According to Eq. (5), longitudinal QPM reciprocal lattice vectors do not depend on the sign of the transverse index m. The structure of the nonlinear lattice under consideration is described by Eq. (1). We determine the Fourier amplitudes of these components for the parameters $C_j = 1$ and $\varphi_j = 0$. In this case (see also [17]), $\eta(y)$ is given by

$$\eta(y) = \mathrm{sgn}[\sin(G_{Y,0}y) + \sin(G_{Y,1}y) + \sin(G_{Y,2}y)]. \tag{6}$$

Figure 3(b) shows the layer thicknesses provided by the function $\eta(y)$ of the layer number in the propagation direction y. The layer thicknesses vary in the range from 8.0 to 12.5 μm, with a mean value of 10.2 μm. It should be noted that this structure could be fabricated using the standard electric-field poling technique [18]. As shown in Fig. 3(c), the Fourier transform of the function $\eta(y)$ contains a triplet of primary spatial frequencies, with the Fourier amplitudes ranging from 0.3 to 0.4. These values of the Fourier amplitudes are consistent with the results found in [17]. The spatial frequencies of these peaks are suitable for the compensation for the wave vector mismatch for the first three NRND orders. Similarly, for the case of a single QPM of the mth NRND order, Eq. (1) reads $\eta(y) = \mathrm{sgn}[\sin(G_{Ym}y)]$. Its Fourier transform is represented as a sharp peak centered at the spatial frequency G_{Ym}, as shown in Fig. 3(c), for the case of a zero order. The corresponding spatial frequency is $G_{Y0} = 0.32\ \mu m^{-1}$ (modulation period $\Lambda = 18.84\ \mu m$), which exactly equals the appropriate wave vector mismatch. As a result, the calculated angular dependence of the second harmonic intensity derived from Eq. (4) grows along the propagation direction for the zero NRND order [Fig. 4(a)]. The second harmonic intensity is four orders of magnitude higher than the maximum second harmonic intensity generated at the coherent length in a 1D lattice. In the same manner, the calculated angular dependence of the second harmonic intensity for the case of multiple QPM grows along the propagation direction for the first three NRND orders [Fig. 4(b)]. The second harmonic intensity is three thousand times higher than the maximum second harmonic intensity generated at the coherent length in a 1D lattice. One can see from

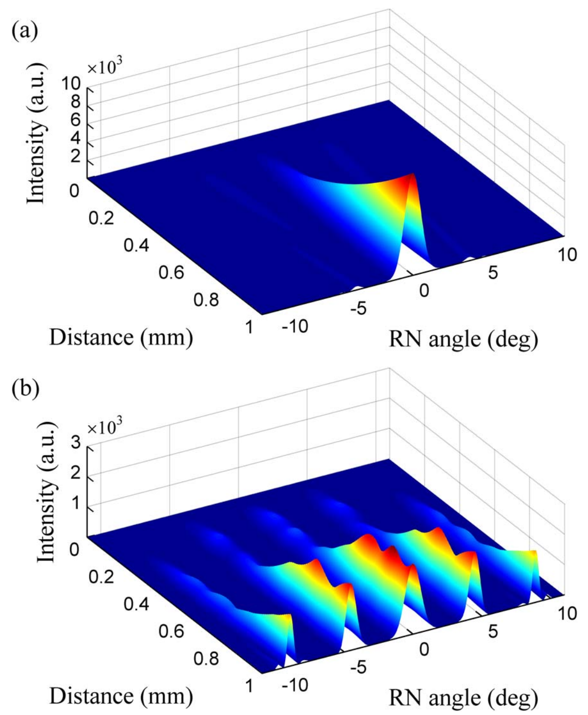

Fig. 4. Evolution of the angular distributions of the second harmonic intensity along the propagation direction for (a) periodic and (b) aperiodic 2D nonlinear photonic lattices shown in Figs. 1(b) and 1(c), respectively.

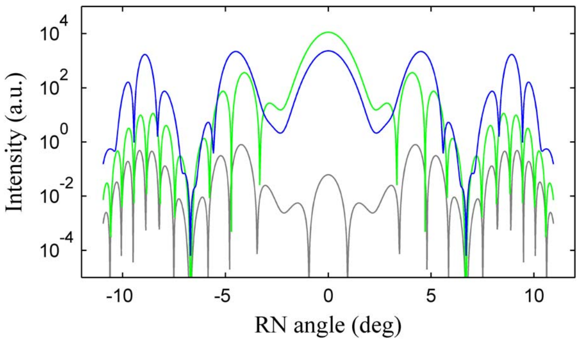

Fig. 5. Resultant angular dependences of second harmonic intensity at the exit from 1D (gray), periodic (green), and aperiodic (blue) 2D nonlinear photonic lattices shown in Fig. 1.

Fig. 4(a) that the monotonic dependence of the second harmonic intensity on the distance is observed for a single QPM interaction. But in the case of multiple QPM interactions, weak spatial modulations of SHG occur due to the contribution of the phase-mismatched interactions, which decrease with the increasing propagation length.

Figure 5 summarizes the resultant angular dependences of the second harmonic intensities generated in 1D, periodic, and aperiodic 2D nonlinear photonic lattices depicted in Fig. 1. These dependences are normalized by the maximum zero-order second harmonic intensity generated at one coherent length in a 1D lattice. One can see that multiple QPM enables us to achieve a remarkable enhancement of SHG and to balance second harmonic intensities between NRND orders. The angular widths are larger than those in the case of a single QPM. Note that the number of periods of second harmonic oscillations falling within the thickness of the lattice is about 50. Therefore, for a shorter wavelength range, we could expect more efficient SHG, due to the shorter periods of the oscillations at the same length of the lattice. On the other hand, the approach developed does not apply the restrictions on the thickness of crystal, and is only restricted by the possibilities of the standard electric-field poling technique [18].

Additionally, the optimization of the duty cycle of the lattice in the transverse direction, the coefficients C_j in Eq. (1), and the length of the lattice in the longitudinal direction provide a wide range of amplitudes of second harmonic beams. The desired intensity distribution between the second harmonic beams can be achieved. The choice of these parameters is a trade-off between efficiency and the number of NRND orders employed.

In summary, we have shown that the method of superposition of quadratic nonlinearity modulation is a powerful tool to design 2D nonlinear photonic lattices providing a desired set of reciprocal lattice vectors suitable for efficient multiple SHG via NRND. The efficiency of this process can be increased by several orders of magnitude compared to the case of nonphase-matched SHG in 1D nonlinear photonic lattices. The proposed approach can be applied to similar calculations in other types of 2D and three-dimensional nonlinear photonic lattices. All that is required is to specify the sequence of the layer thicknesses along the propagation direction. These results open up new possibilities for creating nonlinear multiplexers for the purpose of telecommunication systems, quantum networks, and for optical gratings.

The work was partially supported by the Grant of the President of the Russian Federation MK-2908.2015.2 and by RFBR Grant No. 15-02-03838.

References

1. S. M. Saltiel, D. N. Neshev, R. Fischer, W. Krolikowski, A. Arie, and Y. S. Kivshar, Phys. Rev. Lett. **100**, 103902 (2008).
2. S. M. Saltiel, D. N. Neshev, W. Krolikowski, A. Arie, O. Bang, and Y. S. Kivshar, Opt. Lett. **34**, 848 (2009).
3. K. Kalinowski, P. Roedig, Y. Sheng, M. Ayoub, J. Imbrock, C. Denz, and W. Krolikowski, Opt. Lett. **37**, 1832 (2012).
4. Y. Sheng, W. Wang, R. Shiloh, V. Roppo, A. Arie, and W. Krolikowski, Opt. Lett. **36**, 3266 (2011).
5. Y. Chen, W. Dang, Y. Zheng, X. Chen, and X. Deng, Opt. Lett. **38**, 2298 (2013).
6. A. M. Vyunishev, V. V. Slabko, I. S. Baturin, A. R. Akhmatkhanov, and V. Y. Shur, Opt. Lett. **39**, 4231 (2014).
7. Y. Sheng, Q. Kong, W. Wang, K. Kalinowski, and W. Krolikowski, J. Phys. B **45**, 055401 (2012).
8. V. Berger, Phys. Rev. Lett. **81**, 4136 (1998).
9. Y. Sheng, V. Roppo, Q. Kong, K. Kalinowski, Q. Wang, C. Cojocaru, J. Trull, and W. Krolikowski, Opt. Lett. **36**, 2593 (2011).
10. W. Wang, Y. Sheng, V. Roppo, Z. Chen, X. Niu, and W. Krolikowski, Opt. Express **21**, 18671 (2013).
11. A. A. Novikov and A. S. Chirkin, Zh. Eksp. Teor. Fiz. **133**, 483 (2008) [J. Exp. Theor. Phys. **106**, 415 (2008)].
12. I. V. Shutov, I. A. Ozheredov, A. V. Shumitski, and A. S. Chirkin, Opt. Spectrosc. **105**, 79 (2008).
13. D. H. Jundt, Opt. Lett. **22**, 1553 (1997).
14. M. Baudrier-Raybaut, R. Haïdar, P. Kupecek, P. Lemasson, and E. Rosencher, Nature **432**, 374 (2004).
15. A. S. Aleksandrovsky, A. M. Vyunishev, I. E. Shakhura, A. I. Zaitsev, and A. V. Zamkov, Phys. Rev. A **78**, 031802(R) (2008).
16. A. M. Vyunishev, A. S. Aleksandrovsky, A. I. Zaitsev, A. M. Zhyzhaev, A. V. Shabanov, and V. Petrov, Opt. Lett. **38**, 2691 (2013).
17. A. S. Chirkin and I. V. Shutov, Zh. Eksp. Teor. Fiz. **136**, 639 (2009) [J. Exp. Theor. Phys. **109**, 547 (2009)].
18. V. Y. Shur, J. Mater. Sci. **41**, 199 (2006).